Journal of Constructional Steel Research 137 (2017) 66–76

Contents lists available at ScienceDirect

Journal of Constructional Steel Research

journal homepage: www.elsevier.com/locate/jcsr

Comparison of the moment rotation capacities of rectangular and polygonal hollow sections

John Samuel Kabanda*, ColinMacDougall

Department of Civil Engineering, Queen's University, Kingston K7L 3N6, Canada

ARTICLE INFO

Keywords:
Thin-walled
Hollow structural sections
Local buckling
Web-crippling
Rectangular hollow section (RHS)
Polygonal hollow section (PHS)
Tensile behavior
Residual stress
Stub-column
Four-point bending
Three-point bending
Moment rotation capacity

ABSTRACT

Thin-walled rectangular hollow sections (RHS) have very high torsional rigidity, and thus make a very economic choice for applications which are susceptible to lateral torsional buckling. However, as the depth of a thin-walled RHS increases to ensure adequate bending stiffness, its depth-to-thickness ratio increases and the section is now susceptible to web-crippling/local buckling failure. This causes a reduction in its moment rotation capacity. Therefore, deep thin-walled RHS are not efficient when used as long un-braced spans that require high bending strength and rotation capacity. As such, a new polygonal hollow section (PHS) is proposed. This paper compares the moment rotation capacities of the proposed PHS to those of typical RHS via an experimental program comprising four-point and three-point bending tests. A total of 12 bending tests were conducted and the results showed that the proposed PHS has almost four times the moment rotation capacity of a comparable RHS and the potential to minimize web-crippling failure.

1. Introduction

In the construction industry, long un-braced beams are susceptible to lateral-torsional buckling [1]. As such, hollow structural sections (HSS) are an obvious choice due to their high torsional rigidity, and typically rectangular hollow sections (RHS) are used. However, as the depth of a RHS increases to ensure adequate bending stiffness, there is a tendency for its thin web to become unstable, undergo web-crippling, and exhibit a reduced moment rotation capacity.

Research on web crippling failure in thin-walled HSS members subjected to bending is limited. Elliptical hollow sections (EHS) have been proposed as a solution to web crippling while achieving high bending and torsional stiffness [2]. However, a disadvantage of the EHS is that its curved shape requires specialized manufacturing expertise, especially for welded sections. Furthermore, the resistance of the cross-section depends on calculating its 'equivalent diameter', which is dependent on the location of initiation of buckling and thus also depends on the loading case. As a result, a simpler section that can be categorized as a polygonal hollow section (PHS) is proposed.

The proposed PHS, Fig. 1, approximates an oval hollow section (OHS) and a basic RHS but includes discrete bends in its web and flange [3], which are easier to fabricate than a smoothly curved cross-section. The discrete bends are not only intended to reduce the potential for web crippling, but also help minimize the area of the cross-section and thus result in a marginally lighter beam. Furthermore, the corners of the flanges of the PHS maintain a minimum radius of 3t, where t is the wall thickness. This potentially increases the moment rotation capacity, and also ensures that no microscopic stress cracks and brittle-type failures occur during galvanizing.

There is limited research on PHS in the extant literature and there is also a lack of proper design guidance hindering more widespread use in the industry. In one of the most recent studies, Yamashita et al., 2003 [4] only considered the crush behavior of short polygonal stub-columns (200 mm long) under axial compression. In this paper, the moment rotation capacities of the proposed PHS are compared to those of typical RHS of similar dimensions via an experimental program comprising four-point bending and three-point bending tests.

2. PHS and RHS specimens

A total of 16 specimens (4 stub-columns and 12 beams), which consisted of 8 PHS and 8 RHS of varying lengths, were fabricated. The nominal dimensions, including the moment of inertia I, of the 4 cross-sections used to construct the PHS and RHS specimens are given in Table 1. The dimensions of the PHS are further listed in Table 2. The RHS were fabricated with a single seam weld on the web of the cross-

* Corresponding author.
E-mail address: 14jsk3@queensu.ca (J.S. Kabanda).

http://dx.doi.org/10.1016/j.jcsr.2017.06.005
Received 7 March 2017; Received in revised form 2 June 2017; Accepted 12 June 2017

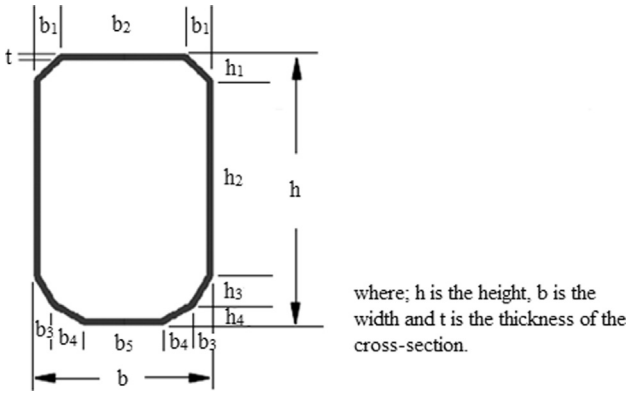

Fig. 1. Illustration of the proposed PHS.

Table 1
Nominal dimensions of the cross-sections of the RHS and PHS.

Cross-section	h(mm)	b(mm)	t(mm)	I(*10^6 mm^4)	b/t	ω_o(mm)
RHS305	305	203	6.4	76	31.7 (Class 3)	0.71
RHS356	356	254	6.4	129	39.7 (Class 4)	0.97
PHS305	305	203	6.4	65	N/A	0.91
PHS356	356	203	6.4	109	N/A	1.01

Table 2
Dimensions of the PHS.

Dimension (Fig. 1)	PHS 305 (mm)	PHS 356 (mm)
b	203	254
b_1	49.5	62
b_2	104	130
b_3	33.5	42
b_4	42	53
b_5	52	64
h	305	356
h_1	57	66
h_2	191	223
h_3	39.6	46
h_4	17.4	21
t	6.4	6.4

section while the PHS had seam welds on the top and bottom flanges of the cross-section. The specimens were all cold-formed members with ASTM A500 (Grade C) steel. The RHS were Class 3 or 4 as per the Canadian steel design standard (CAN/CSA-S16-14) [5] while there is currently no similar classification for the proposed PHS.

Prior to the bending tests, the dimensions and material properties of the 4 cross-sections listed in Table 1 were examined via experimental investigations consisting of geometric imperfection measurements, tensile coupon tests, residual stress analyses and stub column tests.

2.1. Geometric imperfection measurements

During fabrication, distortion of the specimens due to the cold-forming process and welding was minimized. Nevertheless, initial geometric imperfections still exist. Geometric imperfections can affect the moment and rotation capacity of a specimen [7].

In this study, the geometric imperfections were carefully measured along all of the faces of the PHS305, PHS356, RHS305 and RHS356 representative sections using an edge ScanArm. The representative sections were chosen at mid-length and at two locations 80 mm from the specimen ends. Each representative section was mounted on a flat table, and the ScanArm moved continuously around the faces following a specified path, conscientiously guided by a technician to ensure accuracy. The recorded data points were used to determine the

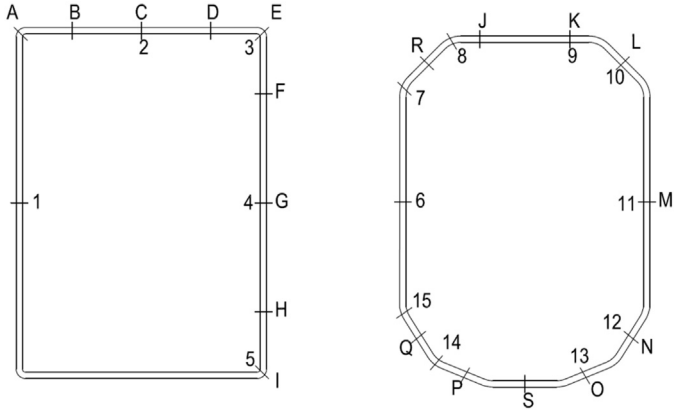

Fig. 2. Locations of the extracted coupons and residual stress measurements.

imperfection amplitude ω_o, which is the difference between the recorded and nominal dimensions. The values listed in Table 1 are the highest ω_o calculated for each representative section and are all within the permitted limits of the ASTM A500 Standard [6].

2.2. Tensile coupon tests

The tensile stress-strain properties along the faces of the PHS305, PHS356, RHS305, and RHS356 were obtained through tensile coupon tests. The coupons were cut from the same length of tubes as the stub-column and beam specimens that will be described in the following sections. Using an Instron 250 kN hydraulic testing machine, a total of 30 tensile tests were completed. The coupons were prepared and tested in accordance with the ASTM A370 standard [8]. For the RHS specimens, three flat coupons at locations 1, 2 and 4; and two corner coupons at locations 3 and 5 were extracted, Fig. 2. For the PHS specimens, six flat coupons at locations 6, 9, 10, 11, 12 and 13; and four corner coupons at locations 7, 8, 14 and 15 were extracted, Fig. 2. A strain gauge was mounted at the centre of each coupon.

Before conducting the tensile coupon tests, it was observed that the shoulders of four of the coupons were curved after extraction. This is due to the release of longitudinal residual stresses, and the shoulders of these coupons were straightened using a hydraulic bending press to allow them to be gripped by the Instron hydraulic testing machine [9].

The key average results from the tensile coupon tests, and the corresponding nominal (mill certificate) properties of the investigated specimens are listed in Table 3; where f_y, and f_u are the yield and ultimate strengths of the materials, respectively and E denotes Young's modulus. Typical measured stress-strain curves from the PHS and RHS specimens are also shown in Fig. 3. The curves exhibit a smooth transition between linear behavior and the yield point, defined as the 0.2% offset stress, typical of cold-formed steel.

2.3. Residual stress measurements

During preparation of the coupons, a few of the extracted coupons were observed to curve away from their initial geometry. This is due to the presence of through-thickness bending residual stresses, common in

Table 3
Nominal$_{(nom)}$and experimental$_{(exp)}$tensile material properties of the PHS and RHS.

Cross-section	$f_{y,nom}$(MPa)	$f_{u,nom}$(MPa)	$f_{y,exp.}$(MPa)	$f_{u,exp.}$(MPa)	$E_{,exp.}$(MPa)
RHS305	423	478	398	425	202,547
RHS356	486	523	448	494	206,384
PHS305	517	564	513	541	205,610
PHS356	573	521	515	547	209,789